

Permeability of sintered microfibrinous composites for heterogeneous catalysis and other chemical processing opportunities

Donald R. Cahela, Bruce J. Tatarchuk*

Chemical Engineering Department, Auburn University, 230 Rose Hall, Auburn, AL 36849, USA

Abstract

Microstructured materials have potential for enhanced mass and heat transfer compared to typical catalyst particulates used in industrial processes. The pressure drop through catalyst-containing materials is a very important reactor design consideration. A model equation to predict porous media permeability (PMP) over the entire range of possible bed voidages is extended to predict properties of sintered metal meshes. A correlation of data for sintered meshes of nickel fibers is presented in the form of a Kozeny constant form drag plot. Comparison of predictions by the PMP equation with data taken on a sintered composite fiber/particle mesh is presented. Use of the PMP equation as a design tool for optimization of media for adsorbents, catalysts, and filters is discussed. © 2001 Elsevier Science B.V. All rights reserved.

Keywords: Permeability; Heterogeneous catalyst; Catalysis; PMP

1. Introduction

A new-patented class of composites materials made by a wet lay paper-making/sintering process can incorporate particles as small as 10 μm into a micrometal fiber matrix [1–4]. Sintered microfibrinous composites using a 16% Ni/alumina catalyst for toluene hydrogenation in a trickle bed reactor have demonstrated 2–6 times higher specific activities than conventional packed bed catalysts on a gravimetric basis, while volumetric activities of 40 vol.% composite catalysts were 80% higher than conventional extrudates [5]. Effectiveness factors for reactions employing such small particles are typically close to unity. The high

thermal conductivity of the micrometal fiber matrix produces radial heat transfer coefficients that are about twice those in packed beds. Enhanced heat transfer due to the larger surface to volume ratio of small particles and the micrometal matrix results in more nearly isothermal conditions in fixed bed reactors minimizing hot spots, resulting in higher selectivity, and allowing processing to be done with smaller safety factors. The micrometal fiber matrix also acts as a micron scale static mixer eliminating channeling. The wet lay paper-making/sintering process allows continuous adjustment of void volume from upwards of 98% down to values similar to packed beds of particles [6]. This allows the composite catalyst/adsorbent material to be optimized to the appropriate void volume for different types of applications. Production of these materials is based on standard paper-making techniques [7], which can be scaled up to manufacturing on high speed continuous paper machines resulting in relatively

* Corresponding author. Tel.: +1-334-844-2023;
fax: +1-334-844-2065.
E-mail addresses: tatarbj@auburn.edu, brucet@eng.auburn.edu
(B.J. Tatarchuk).

Nomenclature

a	wetted surface per volume of bed (cm^2/cm^3)
a_v	surface to volume ratio of a solid shape (cm^2/cm^3)
b/a	aspect ratio of an ellipse
C_D	coefficient of drag for sphere in turbulent flow = 0.6
C_f	coefficient of friction for turbulent flow
C_{FD}	coefficient of form drag of sphere in turbulent flow ($C_{FD} = C_D - C_f$)
D	diameter of characteristic size of any arbitrary shape (cm)
k	Kozeny constant (Eq. (2))
L	geometrical unit cell spacing
ΔP	pressure drop across fixed bed (g/cm^2) or ($\text{cm H}_2\text{O}$)
T	bed thickness (cm)
v_0	face velocity (cm/s)
x_{FD}	form drag parameter, $x_{FD} = \varepsilon^2/12(1 - \varepsilon)$
x_i	volume fractions of components in bed of solids

Greek symbols

α	solid volume fraction, $1 - \varepsilon$
ε	void fraction of bed
θ	angle of flow paths through bed ($^\circ$)
μ	fluid viscosity (P) or ($\text{g}/\text{cm s}$)
ρ	fluid density (gm/cm^3)
τ	tortuosity of cubic cell with one sphere inside, $\tau = 1 + \frac{1}{2}\alpha$
ϕ	shape factor for any arbitrary shape, $\phi = 6/Da_v$

inexpensive materials. For an example of these microfibrous composite carriers, an SEM image of 55–88 μm activated carbon particles entrapped in a micrometal fiber matrix of 2, 4 and 8 μm nickel fibers is shown in Fig. 1.

Dullien [8] reviewed over 300 studies published since 1927 dealing with the permeability of porous media, such as packed beds. None of these studies produced models to predict the permeability of porous media over the entire range of possible void volumes. Ergun's equation, which is fitted to data for packed beds of particulates, is typically used to predict permeability of porous media. Experimental data deviate

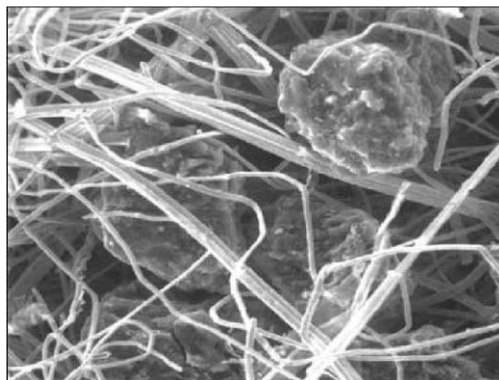


Fig. 1. SEM of sintered composite material of 55–88 μm activated carbon and 2, 4 and 8 μm nickel fibers.

sharply from this equation at void volumes greater than 80%, because it does not account for form drag. The viscous loss portion of Ergun's equation is referred to as the Carman–Kozney equation. Porosity functions have typically been used to empirically correct the Carman–Kozney equation for fibrous media at high voidages where it becomes inaccurate. Several more complicated formulas have been developed for fibrous media, but they lose accuracy at low void volumes, and none of these formulas can be applied directly to mixtures of fibers and particulates. A new theoretically based porous media permeability (PMP) equation, having a single media-dependent parameter, describes permeability across the entire range of void volumes, and is applicable to mixtures of objects of any arbitrary shape.

Almost every process uses porous media. Some examples are: fixed bed reactors, packed distillation columns, adsorbent beds, filters, heat pipes, etc. Equations which predict permeability or pressure drop through the porous media are available, but all of them apply only over a restricted range of porosity, either low porosities or porosities approaching unity. Macdonald et al. [9] reviewed equations describing flow through porous media, and concluded that there are no generally applicable equations. The Ergun equation is the best known, but it is only applicable to media of 50% or less porosity. Kyan et al. [10] developed a pressure drop equation based on a geometrical model, but it is only applicable to high porosity. Their model is unnecessarily complicated, and includes a

deflection energy loss term that is not well justified. In this paper, we develop a generally applicable equation for the permeability of porous media by combining the friction losses estimated by the Hagen–Poiseuille equation, and the form drag losses estimated from Stokes' law.

The equation developed here applies directly to a new class of materials. These materials are fixed beds of micron-sized metal fibers with entrapped particles. Tatarchuk et al. [1–7] developed a method for making these materials based on paper-making technology. Materials are mixed in solution and cast on a screen forming a paper preform. The most basic preform consists of micron-sized metal fibers mixed with cellulose, which acts as a binder in the preform. Preforms are heated in a reducing environment at temperatures from 1073 to 1373 K sintering the metal fibers and gasifying the cellulose. Sintering produces welded joints between the metal fibers resulting in a very mechanically robust material. Fibers of very different properties such as activated carbon or ceramic fibers can be easily incorporated into the paper-making step. Particles can also be added in the paper-making process, so this becomes a very flexible manufacturing process in which materials of vastly different properties can be combined, so the advantageous properties of each material can be accessed in a manner previously unattainable. Previously, a stacked screen model has been used to estimate the permeability of a microfibrinous mesh [5], but this method cannot be easily extended to mixtures of fibers and particles. Permeability of this new class of materials can be estimated by the PMP equation developed here. The PMP equation is also applicable to beds packed to any void fraction and fluidized beds.

2. Porous media permeability equation

Filter materials are composed of fibrous materials and usually have a very high porosity greater than 80%. Usual design equations, such as the Ergun equation, for packed columns do not apply to beds with porosity >50%. The reason these equations cannot be used for high porosity materials is that they do not include the form drag losses, which are small in packing material of low porosity.

Kozeny [11] first developed an equation describing viscous friction losses for flow through packed beds

by considering the packed bed as a collection of capillaries. In Kozeny's model the hydraulic radius of the porous media is inserted into the Hagen–Poiseuille formula for laminar flow inside a pipe. Ergun correlated several hundred data points taken on packed beds to improve the coefficients for the viscous losses in Kozeny's expression, and also fit the coefficient of Burke and Plummer's equation for inertial losses. Bird et al. [12] give a derivation of Ergun's equation for pressure drop in a packed column. Calculating the viscous form drag losses of the porous media by Stokes law, and adding these to the viscous friction losses can improve the Kozeny/Ergun equation for high voidage materials. The resulting PMP equation [13] is given by the following equation for a homogeneous material.

$$\left(\frac{\Delta P}{L}\right)_{\text{Losses}}^{\text{Viscous}} = 72 \frac{\tau^2}{\cos^2(\theta)} \frac{\mu v_0}{\varepsilon^3} \frac{(1 - \varepsilon)^2}{(\phi D)^2} [1 + x_{\text{FD}}] \quad (1)$$

The model parameters are defined in the nomenclature. The angle of flow paths in the permeable media is the only adjustable parameter varying from 0° to 45°, thus allowing only a twofold adjustment in the calculated permeability. The form drag parameter ($x_{\text{FD}} = \varepsilon^2/12(1 - \varepsilon)$) is the ratio of viscous form drag losses to viscous skin friction losses for a homogeneous media. The tortuosity ($\tau = 1 + \frac{1}{2}\alpha$) is estimated for the PMP equation by considering a cubic unit cell containing one spherical particle. Taking this geometrical model and calculating the extra length fluid has to traverse because of the flow around the sphere allows estimation of the tortuosity. This approach results in a very simple result of the tortuosity being unity plus the solid volume fraction divided by 2. The Kozeny constant (k) is a rearrangement of the pressure drop equation for viscous losses intended to eliminate effects of bed porosity and particle size and shape effects. Kozeny constant corresponding to the PMP equation for a homogeneous material is given by the following formula:

$$k \equiv \frac{\Delta P}{L} \frac{1}{\mu v_0} \frac{\varepsilon^3}{(1 - \varepsilon)^2} \left(\frac{\phi D}{6}\right)^2 = \frac{2\tau^2}{\cos^2(\theta)} [1 + x_{\text{FD}}] \quad (2)$$

The derivation of the PMP equation was presented at IEF2000 and is in press [13]. Comparisons of the

PMP equation to literature data taken on textile fibers by Lord [14] and also data tabulated by Jackson and James [15] was also given in the previous publication. Excellent agreement of the PMP equation with the literature data was shown. The data from Jackson et al. extended the range of solid fraction covered down to 3.45×10^{-4} or a form drag parameter of 240, covering three and one-half decades of the form drag parameter. Data for permeability from the highest solid fractions, similar to packed beds, to the lowest solid fractions follow the trend of the PMP equation.

The inertial friction and form drag losses can be estimated by friction factor correlations for turbulent flow as in the derivation of Ergun's equation. Inertial form drag losses can be estimated similarly by a friction factor correlation for a sphere in turbulent flow. The coefficient of form drag is the coefficient of drag minus the coefficient of friction. The drag coefficient for a sphere in turbulent flow is approximately 0.6. The total pressure loss is given by the following equation:

$$\frac{\Delta P}{T} = 72 \frac{\tau^2}{\cos^2(\theta)} \frac{\mu v_0}{\varepsilon^3} \left(\frac{1 - \varepsilon}{\phi D} \right)^2 (1 + x_{FD}) + 6 \frac{\tau^3}{\cos^3(\theta)} \frac{\rho v_0^2}{2\varepsilon^3} \frac{(1 - \varepsilon)}{\phi D} \left(C_f + \frac{C_{FD}}{4} \varepsilon \right) \quad (3)$$

The PMP equation can be generalized to mixtures of any shape by determining the hydraulic radius of the mixture and summing the viscous form drag losses over all of the solid shapes in the composite material. The total pressure drop for a mixture of solid particles or fibers of any shape is given by the following equation:

$$\frac{\Delta P}{T} = 72 \frac{\tau^2}{\cos^2(\theta)} \frac{\mu v_0 (1 - \varepsilon)^2}{\varepsilon^3} \times \left[\left(\sum \frac{x_i}{\phi_i D_i} \right)^2 + x_{FD} \sum \frac{x_i}{(\phi_i D_i)^2} \right] + 6 \frac{\tau^3}{\cos^3(\theta)} \frac{\rho v_0^2}{2} \frac{(1 - \varepsilon)}{\varepsilon^3} \times \left[C_f + C_{FD} \frac{\varepsilon}{4} \right] \sum \frac{x_i}{\phi_i D_i} \quad (4)$$

Parameter values corresponding to the Ergun equation can be found by equating the Ergun equation and the modified Ergun (M-E) equation to the one developed here. Macdonald et al. [9] fitted a very large amount

of data to the M-E and determined best values of the constants in the M-E equation. Values of angle of flow path and coefficient of friction for the PMP equation to equal the M-E at an average bed voidage of 45% are flow path angle of 35° and coefficient of friction of 0.20–0.54.

3. Pressure drop for meshes of sintered composite meshes of metal fibers and particles

3.1. Experimental methods

Nickel fibers of 2, 4, 8 and 12 μm from Micrometals were formed into preforms by standard paper-making methods using 12 g of metal and 3 g of cellulose in a 1 ft² preform. Preparation of these types of materials has been presented previously [1–7]. Rectangular pieces 2.5 cm \times 7.0 cm were sintered at 1223 K with 300 cm³ H₂/min for 1 h, oxidized with 50% air/helium mixture at 773 K for 1 h, and resintered at 1223 K for 1 h. The oxidation step removes all traces of pyrolyzed cellulose from the metal meshes. The nickel meshes typically have a voidage of about 95% after sintering. Twelve three-quarter inch circles were cut out of each of the sintered meshes. These were compressed by various amounts to obtain 10–12 samples with solid volume fractions corresponding to a spread of form drag parameters on the x -axis of the Kozeny constant plots. An SEM image of a sintered mesh of 4 μm nickel fibers is shown in Fig. 2.

Pressure drop through each of the samples was measured using a sample cell consisting of a $\frac{3}{4}$ in.

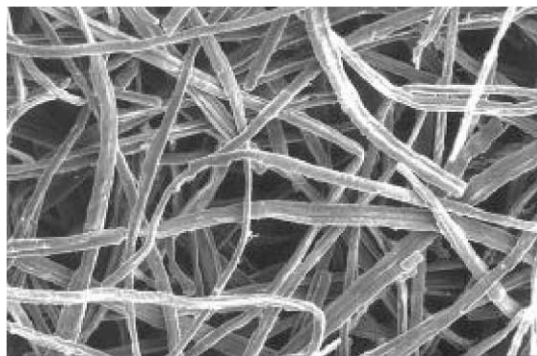


Fig. 2. SEM of mesh of 4 μm nickel fibers.

Swagelok Ultratorr fitting with $\frac{3}{4}$ in. SS tubing inserted into the ends of the Ultratorr fitting. Three-quarter inch OD spacers with $\frac{5}{8}$ in. ID were machined from $\frac{1}{8}$ in. thick aluminum. Two spacers were placed between the sample and the tubing inserted into the sample cell. Connection to an air cylinder with regulator was made through $\frac{1}{4}$ in. SS tubing. A clamp was put around the outside of the sample holder to compress the spacer rings and prevent air from bypassing the sample. A Cole-Parmer flow tube (NO34-39) 0.5–15 l/min, was used to measure the flow rate of air through the sample. The flow tube was calibrated using a 1000 cm³ bubble meter. Pressure drop was measured by a DP cell (OMEGA PX154-010DI), and readings were indicated by a four digit process meter (OMEGA DP24E). The DP cell was calibrated from 0 to 1 in. H₂O using a Dwyer inclined manometer.

For each of the samples pressure drop was measured at 15 flow rates. A Kozney constant form drag plot for these four sets of samples is shown in Fig. 3. Meshes composed of 8 μ m nickel fibers, 100–120 mesh activated carbon powders, and pyrolyzed cellulose were prepared to test against the prediction of the PMP equation. Results of four measurements of permeability against face velocity on meshes compressed from 33 to 69 solid volume percent are shown in Fig. 4A. Values of permeability at 1 cm/s face velocity was

determined by a curve fit of the data, and are plotted against the prediction of the PMP equation as a function of solid volume fraction in Fig. 4B.

3.2. Shape factor of sintered mesh of elliptical fibers

Fibers from Micrometals are described by the manufacturer as ribbon-shaped fibers with an aspect ratio of 3. The fibers appear to be more of an elliptical shape. The 8 and 12 μ m fibers also have ridges that are about $\frac{1}{8}$ as high as the diameter of the fibers discernable in the SEM images. To calculate Kozeny constants for these samples a shape factor for the sintered meshes is required. The shape factor for an elliptical fiber can easily be calculated from formulas for the area and perimeter of an ellipse [16]. Many different geometrical cell models can describe a mesh of sintered fibers. The model which will be used to estimate the shape factor of sintered meshes of metal fibers is a geometrical model of layers of fibers separated equidistantly in space which are stacked at right angles to each other. Each set of two perpendicular layers are separated by the same distance as the spacing between fibers in each layer. Considering the overlapping areas of the fibers as lost during the sintering process allows estimation of the

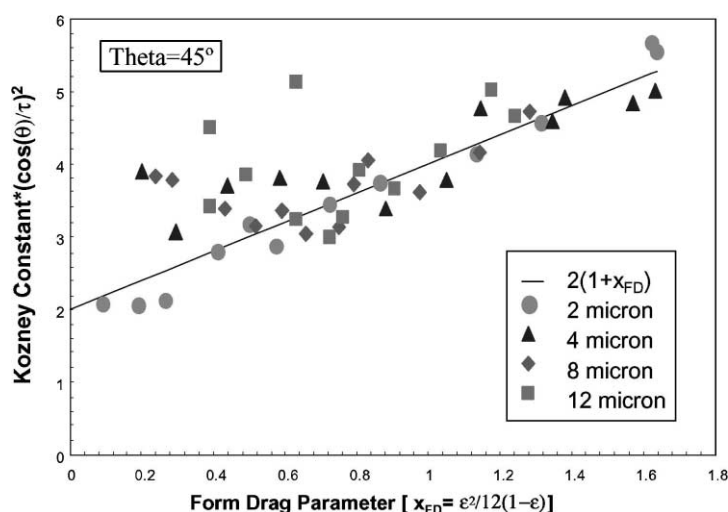


Fig. 3. Kozney constant form drag plot of data for meshes of 2, 4, 8 and 12 μ m micrometals nickel fibers.

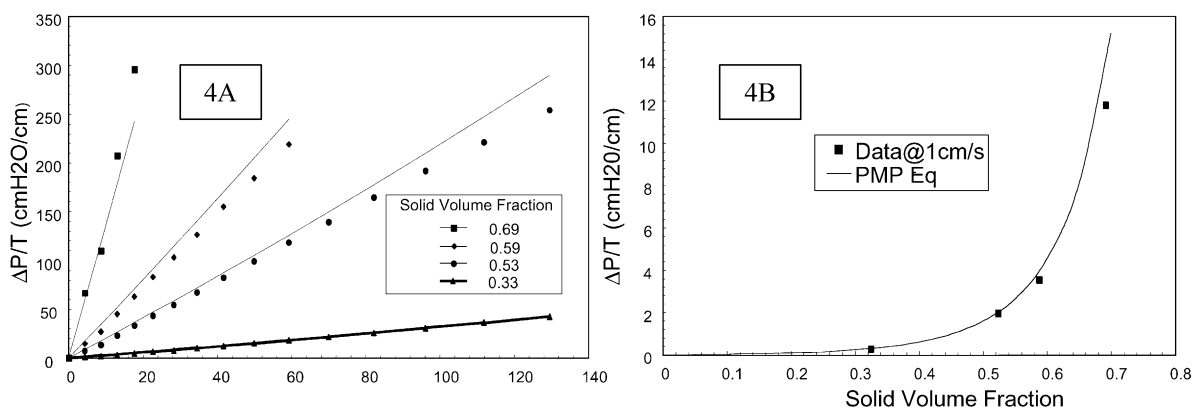


Fig. 4. (A and B) Pressure drop through 8 μm nickel fiber/ACP meshes with comparison to PMP equation 8 μm nickel fibers, 100–120 mesh Calgon BPL, and 10 μm PC remnants; solid volume percentages of nickel, ACP and PC of: 7.1, 91.4 and 1.5 μm . Fiber diameters used in PMP for nickel, ACP, and PC of: 7.6, 137 and 10.4 μm . Flow path angle of 20° was used.

shape factor of a sintered mesh. The shape factor for this model is given by the following formula:

$$\phi_{\text{MEF}} = \frac{3\sqrt{b/a}}{[2 - \sqrt{(2(b/a)\alpha_M)/\pi}]\sqrt{(1 + (b/a)^2)/2}} \quad (5)$$

For a solid fraction of zero this formula reduces to the shape factor of an elliptical fiber, and for an aspect ratio of 1 it reduces further to a value of $\frac{3}{2}$, which is the shape factor for a cylindrical fiber.

The hydrodynamic diameter which is the value which best fit the permeability data best with a flow path angle of 45° was used in the Kozeny constant form drag plot. The hydrodynamic diameters are close to the average diameters calculated from the area of an ellipse, but slightly smaller for 8 and 12 μm fibers. The hydrodynamic diameters used for nominal 2, 4, 8 and 12 μm fibers were 2.30, 3.50, 7.60 and 9.85 μm . These fibers all exhibit about 12 ridges with a height about $\frac{1}{8}$ the width of the fibers. These ridges can easily explain the slightly smaller diameter required to fit the permeability data by calculating a shape factor for a rough fiber model and calculating an equivalent smooth fiber diameter with a shape factor of 1.5. The details of this comparison will be omitted. A Kozeny constant form drag plot for 2, 4, 8 and 12 μm nickel fibers meshes is shown in Fig. 3. The permeability data for 2 μm nickel fiber meshes, shown as solid circles, conform to the theoretical curve for all form drag

parameters within about 10%. Kozeny constants for 4, 8 and 12 μm fibers show a scatter of about 10% for form drag parameters >0.7 corresponding to a solid volume fraction of 10% or a void volume of 90%. The scatter in the data is likely due to errors in measuring sample thickness for thin layers used in these measurements. Using thick plugs of material would eliminate errors in the bed thickness measurements. For higher solid volume fractions the data tends to be above the theoretical line in the Kozeny constant form drag plot. These points correspond to predicted pressure drops that are lower than the experimental data. The predicted pressure drop is lower than the data due to loss of surface area not being as large as predicted by the shape factor for a sintered mesh of elliptical fibers for solid volume fractions greater than 10%. If meshes compacted to solid volume fractions greater than 10% were sintered again, the pressure drop through them would likely be much smaller than that through the meshes sintered only once. This lower pressure drop would result from loss of surface area due to sintering of contact points between fibers. So, the shape factor for sintered meshes of elliptical fibers given here does not well represent meshes of metal fibers sintered once and compacted to more than 10% solid volume fraction.

Permeability for meshes composed of 8 μm nickel fibers, 100–120 mesh activated carbon powders (ACP), and pyrolyzed cellulose (PC) and the prediction of using the PMP equation show a very good

agreement in Fig. 4 for the four samples measured. The shape factor for a sintered metal mesh was used for the nickel fibers in the composite meshes based on the solid volume fraction of the nickel component. Shape factors for the ACP and PC were considered as constant at 0.72 and 1.5. A flow path angle of 20° was used in the prediction by the PMP equation for the composite meshes.

4. Optimization of adsorbent material using the PMP equation

Previously there has not been a modeling tool available to calculate pressure drop through mixtures of fibers and particles, so an optimization of an adsorbent material for adsorption properties and pressure drop had to be done solely by experimentation. Combining this model with a prediction of the concentration breakthrough allows for prediction of the optimum size of the adsorbent particles. The adsorption rate constant for a mass transfer limited adsorption is inversely proportional to the square of the particle diameter, and the pressure drop is proportional to the square of the particle diameter. Low pressure drop and high adsorption rate are desired. An optimum particle size which gives minimum pressure drop and minimum amount of adsorbent for a required adsorption capacity can be determined given a breakthrough concentration model such as the Bed Depth Service Time equation first derived by Bohart and Adams [17].

5. Summary

A model equation that predicts PMP over the entire range of possible bed voidages has been extended to predict properties of sintered metal meshes. A correlation of data for sintered meshes of nickel fibers has been presented in the form of a Kozeny form drag plot. Comparison of the PMP equation with data

from a composite fiber/particle mesh has also been presented. Use of this model for optimization of adsorbent meshes was briefly discussed.

Acknowledgements

The authors gratefully acknowledge the financial support of ONR and DARPA through contract ONR N000014-00-10282.

References

- [1] B.J. Tatarchuk, M.R. Rose, A. Krishnagopalan, J.N. Zabasajja, D. Kohler, US Patent 5 080 963.
- [2] B.J. Tatarchuk, US Patent 5 096 663.
- [3] B.J. Tatarchuk, M.F. Rose, A. Krishnagopalan, US Patent 5 102 745.
- [4] B.J. Tatarchuk, M.F. Rose, G.A. Krishnagopalan, J.N. Zabasajja, D.A. Kohler, US Patent 5 304 330.
- [5] M.W. Meffert, Preparation and characterization of sintered metal microfiber-based composite materials for heterogeneous catalyst applications, Ph.D. Thesis, Auburn University, Auburn, AL, 1998.
- [6] C.J. Marrion, D.R. Cahela, S. Ahn, B.J. Tatarchuk, *J. Power Sources* 47 (1994) 297–302.
- [7] D. Kohler, J. Zabasajja, A. Krishnagopalan, B. Tatarchuk, *J. Electrochem. Soc.* 137 (1990) 136.
- [8] F.A.L. Dullien, *Porous Media: Fluid Transport and Pore Structure*, Academic Press, New York, 1992.
- [9] I.F. Macdonald, M.S. El-Sayed, K. Mow, F.A.L. Dullien, *Ind. Eng. Chem. Fund.* 18 (1979) 199.
- [10] C.P. Kyan, D.T. Watson, R.C. Kinter, *Ind. Eng. Chem. Fund.* 9 (1970) 596.
- [11] I.J. Kozeny, *Wasserkraft und Wasserwerischaft* 1 (1931) 67.
- [12] R.B. Bird, W.E. Stewart, E.N. Lightfoot, *Transport Phenomena*, Wiley, New York, 1960, pp. 196–200.
- [13] D.K. Harris, D.R. Cahela, B.J. Tatarchuk, Wet layup and sintering of metal-containing microfibrous composites for chemical processing opportunities, IEF2000, Italy, May 2000 and JCOMA 2001, in press.
- [14] E. Lord, *J. Text. Inst.* 46 (1955) T191.
- [15] G.W. Jackson, D.F. James, *Can. J. Chem. Eng.* 64 (1986) 364.
- [16] W.H. Beyer, S.M. Selby (Eds.), *Standard Mathematical Tables*, 24th Edition, CRC Press, Boca Raton, FL, 1976.
- [17] G.S. Bohart, E.Q. Adams, *J. Am. Chem. Soc.* 42 (1920) 523–544.